Angiogenesis (2019) 22:133–144
https://doi.org/10.1007/s10456-018-9644-3

ORIGINAL PAPER

The calcium-binding type III repeats domain of thrombospondin-2 binds to fibroblast growth factor 2 (FGF2)

Marco Rusnati[1] · Patrizia Borsotti[2] · Elisabetta Moroni[3] · Chiara Foglieni[2,7] · Paola Chiodelli[1] · Laura Carminati[2] · Denise Pinessi[2] · Douglas S. Annis[4] · Giulia Paiardi[1] · Antonella Bugatti[1] · Alessandro Gori[5] · Renato Longhi[5] · Dorina Belotti[2] · Deane F. Mosher[4] · Giorgio Colombo[5,6] · Giulia Taraboletti[2]

Received: 31 May 2018 / Accepted: 16 August 2018 / Published online: 30 August 2018

Abstract

Thrombospondin (TSP)-1 and TSP-2 share similar structures and functions, including a remarkable antiangiogenic activity. We have previously demonstrated that a mechanism of the antiangiogenic activity of TSP-1 is the interaction of its type III repeats domain with fibroblast growth factor-2 (FGF2), affecting the growth factor bioavailability and angiogenic activity. Since the type III repeats domain is conserved in TSP-2, this study aimed at investigating whether also TSP-2 retained the ability to interact with FGF2. The FGF2 binding properties of TSP-1 and TSP-2 and their recombinant domains were analyzed by solid-phase binding and surface plasmon resonance assays. TSP-2 bound FGF2 with high affinity ($Kd = 1.3$ nM). TSP-2/FGF2 binding was inhibited by calcium and heparin. The FGF2-binding domain of TSP-2 was located in the type III repeats and the minimal interacting sequence was identified as the GVTDEKD peptide in repeat 3C, corresponding to KIPDDRD, the active sequence of TSP-1. A second putative FGF2 binding sequence was also identified in repeat 11C of both TSPs. Computational docking analysis predicted that both the TSP-2 and TSP-1-derived heptapeptides interacted with FGF2 with comparable binding properties. Accordingly, small molecules based on the TSP-1 active sequence blocked TSP-2/FGF2 interaction. Binding of TSP-2 to FGF2 impaired the growth factor ability to interact with its cellular receptors, since TSP-2-derived fragments prevented the binding of FGF2 to both heparin (used as a structural analog of heparan sulfate proteoglycans) and FGFR-1. These findings identify TSP-2 as a new FGF2 ligand that shares with TSP-1 the same molecular requirements for interaction with the growth factor and a comparable capacity to block FGF2 interaction with proangiogenic receptors. These features likely contribute to TSP-2 antiangiogenic and antineoplastic activity, providing the rationale for future therapeutic applications.

Keywords Thrombospondins · FGF2 · Angiogenesis · Matricellular proteins

Electronic supplementary material The online version of this article (https://doi.org/10.1007/s10456-018-9644-3) contains supplementary material, which is available to authorized users.

✉ Giulia Taraboletti
giulia.taraboletti@marionegri.it

[1] Section of Experimental Oncology and Immunology, Department of Molecular and Translational Medicine, University of Brescia, Brescia 25123, Italy

[2] Tumor Angiogenesis Unit, Department of Oncology, Istituto di Ricerche Farmacologiche Mario Negri IRCCS, Via Stezzano, 87, Bergamo 24126, Italy

[3] IRCCS MultiMedica, Milano 20138, Italy

[4] Departments of Biomolecular Chemistry and Medicine, University of Wisconsin, Madison, WI 53706, USA

[5] Istituto di Chimica del Riconoscimento Molecolare, Consiglio Nazionale delle Ricerche (ICRM-CNR), Milano 20131, Italy

[6] Dipartimento di Chimica, Università di Pavia, Pavia 27100, Italy

[7] Present Address: Laboratory for Biomedical Neurosciences, Neurocenter of Southern Switzerland, Torricella-Taverne, Switzerland

Introduction

Thrombospondins (TSPs) are a family of five related matricellular glycoproteins. On the basis of their structure, they are classified into two groups: the homotrimeric TSP-1 and TSP-2 and the homopentameric TSP-3, TSP-4, and COMP. The modular structure of TSP-1 and TSP-2 consists of an *N*-terminal heparin-binding domain, an oligomerization domain, followed by a von Willebrand factor type C domain, three properdin-like type I repeats (absent in TSP-3, TSP-4, and COMP), three EGF-like type II repeats, the calcium-binding type III repeats, and a globular, lectin-like *C*-terminal region. The most conserved region among all TSPs is the signature domain that spans from the third type II repeat to the *C*-terminus [1].

In line with their structural similarity, TSP-1 and TSP-2 share many functional properties, including a remarkable antiangiogenic activity (reviewed in [2–4]). TSP-2 is indeed a potent inhibitor of endothelial cell migration and proliferation induced by several angiogenic factors, including FGF2 [5–7] and prevents neovascularization in the rat cornea [5]. Mice lacking TSP-2 display a marked increment of vascular density in the dermis and adipose tissue [8] as well as prolonged neovascularization and accelerated healing of excisional wounds [9]. In keeping with its antiangiogenic activity, TSP-2 has a protective role against tumorigenesis, since susceptibility to skin carcinogenesis was enhanced in TSP-2-deficient mice [10] and decreased in transgenic mice overexpressing TSP-2 in the skin [11]. The expression of TSP-2 in tumors has been correlated with reduced vascularity and a more favorable prognosis in several tumor types including gastric cancer [12], colon cancer [13], non-small cell lung cancer [14], and neuroblastoma [15]. In addition, induced overexpression of TSP-2 resulted in reduced tumorigenesis, vascularity, and metastasis formation in different tumor models [4, 16, 17].

Multiple mechanisms contribute to the antiangiogenic activity of TSP-2 [3, 4] including direct interaction with antiangiogenic receptors and transduction of antiangiogenic signals in endothelial cells. Like TSP-1, TSP-2 interacts with CD36 (through the type I repeats) [18] as well as integrins, heparan sulfate proteoglycans (HSPG), and low-density lipoprotein receptor-related protein. Conversely, unlike TSP-1, CD47 is apparently not involved in the antiangiogenic activity of TSP-2 [19]. The two TSPs regulate angiogenesis also by interacting with extracellular matrix components, serine proteases, and matrix metalloproteinases, particularly MMP-2 and MMP-9, therefore affecting extracellular matrix assembly and remodeling [4, 20]. Finally, TSP-1 and TSP-2 can interact with angiogenic growth factors, regulating their bioavailability and interaction with receptors [3, 4, 21]. We previously reported that TSP-1 directly binds and sequesters the angiogenic factor FGF2, preventing the binding of the growth factor to endothelial cell receptors and the extracellular matrix, hence affecting FGF2 bioavailability and ultimately preventing FGF2-induced angiogenesis [22–24]. We also characterized the TSP-1/FGF2 interaction, demonstrating that a sequence located in the type III repeats of TSP-1 binds with high affinity to the heparin-binding site of FGF2 [23–25].

Given the sequence and structure similarity between the type III repeats of TSP-1 and TSP-2, we hypothesized that also TSP-2 might interact with FGF2. To evaluate this hypothesis, we carried out a comparative study of the two TSPs for their FGF2-binding capacity, using recombinant portions, derived synthetic peptides, and small molecules. Our findings identify TSP-2 as a second member of the TSP family able to interact with FGF2, shedding light on TSP-2 antiangiogenic activity and setting the bases for future development of TSP-2-based inhibitors of FGF2.

Materials and methods

TSPs, TSP recombinant fragments, synthetic peptides, and small molecules

Recombinant human TSP-2 was from R&D Systems (Minneapolis, MN). TSP-1 was purified from thrombin-stimulated human platelets.

Recombinant human TSP-1-derived fragments (E123CaG-1, E3CaG-1, and Ca-1) and TSP-2-derived fragments (E123CaG-2, E3CaG-2, and Ca-2) were expressed in insect cells using baculovirus as previously described [26, 27].

Biotin-labeled TSP-1-derived peptides DD15, DD10, KIP7, KIP5 were from Pepscan (Lelystad, The Netherlands). The other peptides (TSP-1: KIPDDRD and IPDDKD; TSP-2: GVTDEKD and VPDDRD) were synthesized by solid-phase peptide synthesis (SPPS) following a standard Fmoc-protocol [28]. Biotinylated peptides were obtained by incorporating Lys(biotin-ε-aminocaproyl) into the sequences. Upon full chain assembly and cleavage, peptides were isolated to > 95% purity by RP-HPLC.

The TSP-1-based small molecules, inhibitors of FGF2, SM27 (NSC37204), SM.2-16 (NSC45622), and SM.2-20 (NSC58057) [25, 29] were provided by the Developmental Therapeutics Program (DTP), division of Cancer Treatment and Diagnosis, NCI, NIH (USA).

Other reagents

Human recombinant FGF2 (R&D Systems, Minneapolis, MN) was obtained through the NCI-Biological Resources Branch (Frederick, MD).

Labeling of proteins

TSP-2, TSP-1, and their recombinant fragments were biotinylated in PBS (pH 7.4) with biotinamidocaproate-*N*-hydroxysulfo-succinimide ester (Sigma, St. Louis, MO), and the biotinylated molecules were isolated by chromatography on Micro Bio-Spin columns (Bio-Rad Lab, Milan, Italy), as previously described [23, 25].

Solid-phase binding assay

DELFIA® microtitration plates and DELFIA® reagents were from PerkinElmer. Plates were coated overnight at 4 °C with FGF2 in PBS (0.1 µg/40 µl/well). After washing, non-specific binding sites were saturated by a 30-min incubation with PBS 1% BSA. Biotin-labeled TSP-1, TSP-2, recombinant fragments, or synthetic peptides were added in 40 µl PBS 1% BSA with or without the indicated concentration of calcium, heparin, or small molecules, and incubated for 3 h at room temperature. The plates were washed with PBS 0.1% BSA and incubated for 1 h with 100 µl/well Eu-labeled Streptavidin 1:1000 at room temperature. After washing, plates were incubated with DELFIA® Enhancement Solution. Time-resolved fluorescence was measured using a Victor^3 multilabel plate reader (PerkinElmer). Each experiment was repeated at least twice. Data are reported as specific binding (i.e., subtracted non-specific binding to uncoated, BSA-saturated plastic).

SPR analysis

SPR measurements were performed on a BIAcore X100 instrument (GE-Healthcare, WI). FGF2 was immobilized on a CM5 sensorchip (GE-Healthcare) as described [22], allowing the immobilization of 7800 RU resonance units (RU) (430 fmol/mm^2 of FGF2). FGFR-1 was immobilized on a CMD50L sensorchip (Xantec Bioanalytics, Dusseldorf, Germany) as described [30], allowing the immobilization of 3800 RU (42 fmol/mm^2 of FGFR-1). Fragment E123CaG-1 was immobilized as described [23]. Reference surfaces were prepared in parallel with no ligand immobilized (for FGF2 and FGFR-1) or with immobilized BSA (for E123CaG-1). Biotinylated-heparin was immobilized onto a CMD50L sensorchip that was previously activated and coated with streptavidin as described [30], allowing the immobilization of 80 RU (6 fmol/mm^2 of heparin). A streptavidin-coated sensorchip was used for blank subtraction.

To analyze their direct binding to sensorchip-immobilized FGF2, TSP-1, TSP-2, Ca-1, and Ca-2 were resuspended in 10 mM HEPES, 150 mM NaCl, 0.05% surfactant P20, pH 7.4 (HBS-P) at increasing concentrations (from 1.58 to 150 nM for TSPs and from 306 to 9800 nM for the Ca domains), injected for 2 min (to allow their association to FGF2), and washed until dissociation was observed.

For competition experiments, FGF2 (150 nM) was resuspended in HBS-EP in the presence of increasing concentrations of the compounds (from 3 to 1000 nM) and injected over the heparin, FGFR-1 of E123CaG-1 surfaces for 5 min (to allow the association of the growth factor with the surfaces), and washed until dissociation was observed. In both the experimental conditions, the sensorchips were regenerated after every run by injection of glycine 10 mM pH 2.0.

Molecular dynamics simulations and docking calculations

All atom molecular dynamics simulations were carried out on a simulation time scale of 500 ns for both peptides in isolation, using an explicit water model. Three replicas for each peptide were combined and analyses were carried out on the resulting meta-trajectories. The fully extended conformations of the peptides generated with LEaP program were used as starting structure.

The simulations were performed using Amber16 pmemd. CUDA with the all atom ff99SB force field under periodic boundary conditions. In order to remove any bad contacts, every system was first minimized in vacuo by multiple minimizations (200 steps steepest descent plus 200 steps conjugate gradient). The simulative box has been filled with TIP3P water molecules and rendered electroneutral by addition of counterions. It consists of a final number of atoms of ~ 5600 for each system. The systems were then subjected to a round of minimization of 10,000 steps of steepest descend followed by 10,000 steps of conjugate gradient. Relaxation of water molecules and thermalization in NPT environment were carried out for 1.2 ns at 1 fs time-step. In particular, six runs of 200 ps each were carried out increasing the temperature of 50 K at each step, starting from 50 K to 300 K. The systems were then simulated with a 2 fs time-step in periodic boundary conditions in the NVT ensemble. A cutoff of 8 Å for the evaluation of short-range non-bonded interactions and the Particle Mesh Ewald method for the long-range electrostatic interactions have been used. The temperature was kept constant at 300 K with Langevin thermostat. Bonds involving hydrogen atoms were constrained with the SHAKE algorithm.

Analyses were carried out with the tools in the Gromacs 4.6.2 package or with code written in-house.

The most representative structures of both peptides have been determined using the cluster algorithm described by Daura and coworkers, considering the meta-trajectories of both peptides, taking into account of backbones and beta carbons. The algorithm counts the number of neighbors using a cutoff of 0.1 nm for RMSD between the optimal

backbone and C-beta superimposition of the sampled structures, then takes the structure with the largest number of neighbors with all its neighbors as cluster, and eliminates it from the pool of clusters. This procedure is repeated for the remaining structures in the pool. We kept the representative structures of 20 clusters for subsequent analysis, representing ~ 90% of the structure variability of both peptides.

Docking calculations were performed using the program Glide (version-69018) keeping FGF2 (X-ray structure downloaded from the PDB:1fq9) rigid and allowing flexibility for the ligands. Docking calculations were performed in Standard Precision mode (SP) with the OPLS-AA (2001) force field, non-planar conformations of amide bonds were penalized, Van der Waals radii were scaled by 0.80, and the partial charge cutoff was fixed to 0.15. No further modifications were applied to the default settings.

Results

FGF2-binding ability of TSP-2 type III repeats domain

We previously reported that TSP-1 interacts with FGF2 through the type III repeat [23–25]. Since this domain is highly conserved in TSP-2, the other antiangiogenic member of the TSP family, we investigated whether also TSP-2 was able to interact with FGF2. In a solid-phase binding assay, labeled recombinant TSP-2 bound to immobilized FGF2 in a dose-dependent and saturating manner and with a potency similar to that of TSP-1 (Fig. 1a and Suppl Fig. 1). SPR analysis, performed to characterize and compare the binding of the two TSPs to FGF2, confirmed the dose-dependent and saturable nature of the binding of both TSP-2 and TSP-1 to

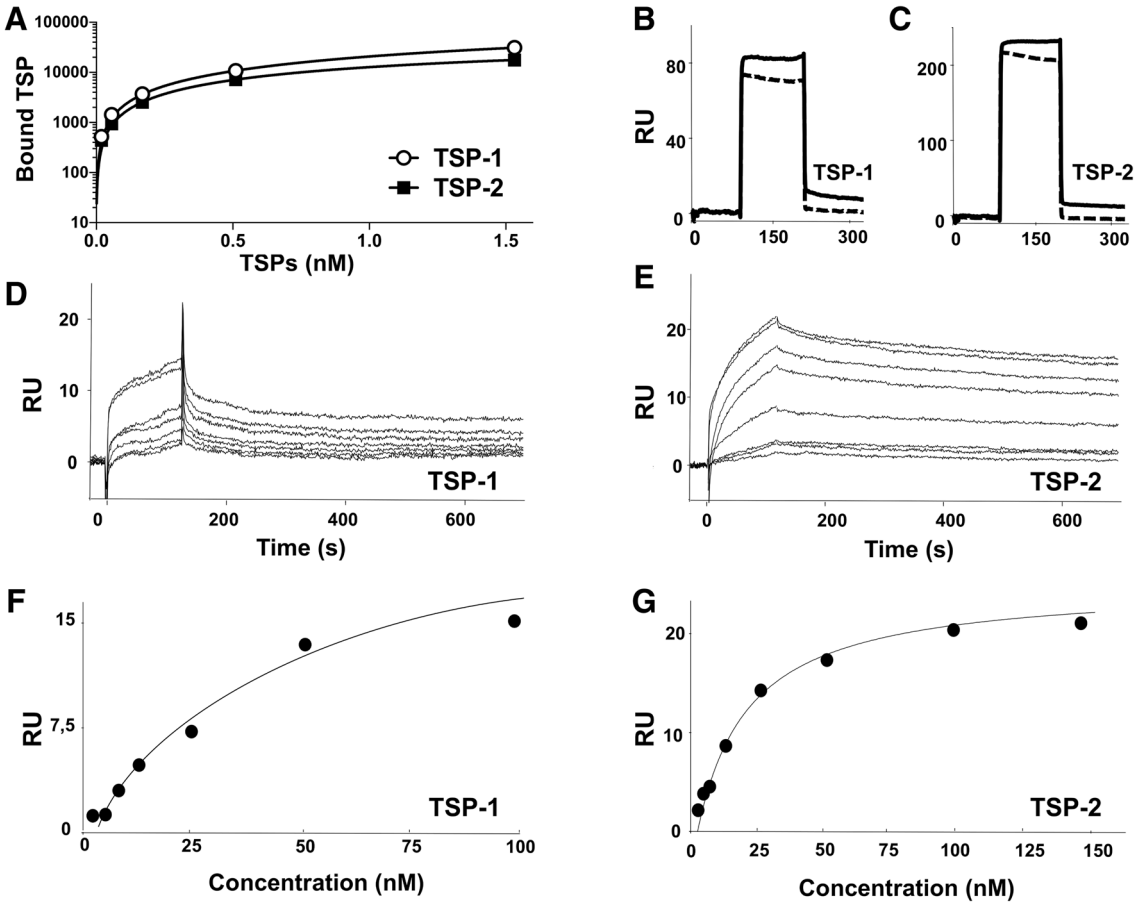

Fig. 1 Binding of TSP-2 and TSP-1 to FGF2. **a** Solid-phase assay: binding of increasing concentrations of biotin-labeled TSP-1 or TSP-2 to immobilized FGF2. Data are expressed as specific binding to FGF2 (absorbance, mean and SD, from one experiment representative of three), after subtraction of non-specific binding to BSA-saturated plastic (shown in Suppl Fig. 1). **b**–**g** SPR analysis: sensorgrams showing the binding of TSP-1 (**b**) or TSP-2 (**c**) (both at 100 nM) to FGF2-coated or void sensorchips (straight and dashed lines, respectively). Representative blank-subtracted sensorgrams overlays showing the binding of increasing concentrations of TSP-1 (**d**) or of TSP-2 (**e**) to the FGF2-coated sensorchip. **f**, **g** Saturation curves obtained using the values of RU bound at equilibrium from injections of increasing concentrations of TSP-1 or TSP-2, respectively, onto the FGF2-coated sensorchip

FGF2 (Fig. 1b–g). Association (K_{on}) and dissociation (K_{off}) rates were similar for the two TSPs (Table 1). Calculation of *Kd* values by means of either the K_{off}/K_{on} ratio or of steady-state analysis obtained by fitting the proper form of Scatchard's equation of the bound RU at equilibrium revealed that the two interactions occurred with a similar and relatively high affinity (*Kd* values in the low nanomolar range, Table 1). In the case of TSP-1, the calculated values were comparable to those previously reported [22].

We next used biotinylated proteins comprising the entire signature domain of TSP-2 (E123CaG-2 fragment) or only the type III repeats (Ca-2) (see Fig. 2a for a schematic representation of the fragments used) to locate the FGF2-binding site of TSP-2. E123CaG-1 and Ca-1, which contain the FGF2 binding sequence of TSP-1 [23], were used as controls. In the solid-phase assay, both E123CaG-2 (Fig. 2b) and Ca-2 (Fig. 2c) bound to FGF2 in a manner undistinguishable from that of the corresponding TSP-1-derived fragments (see also Suppl Fig. 2), thus indicating that also the FGF2-binding site of TSP-2 is located in the type III repeats. FGF2 interaction with TSP-2 type III repeats was confirmed using an inverse experimental approach, where labeled FGF2 was found to bind to plastic-bound Ca-1 and Ca-2 in a similar manner (data not shown).

SPR analysis was then exploited to define the FGF2-binding features of Ca-2 in comparison with Ca-1 (Fig. 2d–i). In the experimental conditions adopted, Ca-2 bound to immobilized FGF2 in a dose-dependent but not-saturating manner, with K_{on} and K_{off} rates similar to those of Ca-1 (Table 1). Calculation of *Kd* value by means of the K_{off}/K_{on} ratio revealed that FGF2 interaction with Ca-2 occurred with an affinity that is significantly lower than that calculated for TSP-2 native protein (*Kd* value in the high nanomolar range) (Table 1). Also, a competition experiment was set up to directly compare the relative affinity of the binding to FGF2 of Ca-1, Ca-2, E123CaG-1, and E123CaG-2 peptides. As shown in Suppl Fig. 3, both the Ca peptides inhibited the binding of FGF2 to immobilized E123CaG-1 with a similar potency (in the high nanomolar range) that is significantly higher than that of the two corresponding E123CaG peptides (similar inhibition, in the low nanomolar range). Taken together, these data confirm that Ca-2 and Ca-1 fragments bind to FGF2 with comparable affinities and point to a direct correlation existing between the length of the TSPs derived fragments and their affinity for FGF2 (intact TSP > E123CaG > Ca). This is in agreement with the described regulatory role of flanking regions on the structure and activity of the type III repeats domain [31, 32].

FGF2/TSP-2 interaction is affected by calcium and heparin

The type III repeats of TSP-1 and TSP-2 bind 26 calcium ions that control the structure of the domain and whether active sequences are exposed or not [33, 34]. We previously found that binding of TSP-1 to FGF2 occurs preferentially at low calcium, when the structure of the type III repeats extends, exposing the FGF2-binding site [23]. Here we found that, in a similar way, calcium inhibited the binding of Ca-2 to FGF2 with an IC_{50} of 0.15 ± 0.05 mM, comparable to that of Ca-1 (0.16 ± 0.01 mM) (Fig. 3a). Increasing calcium concentration also affected the FGF2-binding ability of E123CaG-1 and E123CaG-2, in a similar manner (Suppl Fig. 4). The curves of FGF2 binding versus calcium concentration parallel those generated in studies showing that calcium alters the biophysical properties of Ca-1 in a highly cooperative manner [35, 36], indicating an association between these processes. These data therefore indicate that also in TSP-2 the availability of the FGF2-binding site is calcium-dependent.

TSP-1 interacts with the heparin-binding site of FGF2 [24, 25]. To assess if also TSP-2 recognizes the heparin-binding region in FGF2, we evaluated the effect of free heparin on the binding of Ca-2 to FGF2. As shown in Fig. 3b, free heparin inhibited the binding of Ca-2 and Ca-1 (used as a control) to FGF2, suggesting that TSP-2 binds to FGF2 through the heparin-binding site of the growth factor.

Table 1 Binding parameters of the interactions of TSP-1, TSP-2, Ca-1, and Ca-2 with FGF2 immobilized to a BIAcore sensorchip

Ligand	K_{on} (1/Ms)	K_{off} (1/s)	Kd_{kin} (nM)	Kd_{eq} (nM)
TSP-1	$4.9 \times 10^5 \pm 1.6 \times 10^5$	$9.7 \times 10^{-4} \pm 1.4 \times 10^{-4}$	4.88 ± 1.4	28.0 ± 4.5
TSP-2	$2.6 \times 10^5 \pm 0.3 \times 10^5$	$3.4 \times 10^{-4} \pm 0.8 \times 10^{-4}$	1.27 ± 0.2	15.1 ± 4.2
Ca-1	$1.1 \times 10^3 \pm 0.4 \times 10^3$	$4.7 \times 10^{-4} \pm 0.3 \times 10^{-4}$	520 ± 180	*ND*
Ca-2	$7.9 \times 10^3 \pm 2.6 \times 10^3$	$6.5 \times 10^{-4} \pm 0.7 \times 10^{-4}$	911 ± 526	*ND*

Association rate (K_{on}), dissociation rate (K_{off}), and the dissociation constant (*Kd*) derived from the K_{off}/K_{on} ratio (Kd_{kin}) or from Scatchard plot analysis of the equilibrium binding data (Kd_{eq}) are reported. The results shown are the mean ± SD of 3–4 independent analysis

ND not determinable

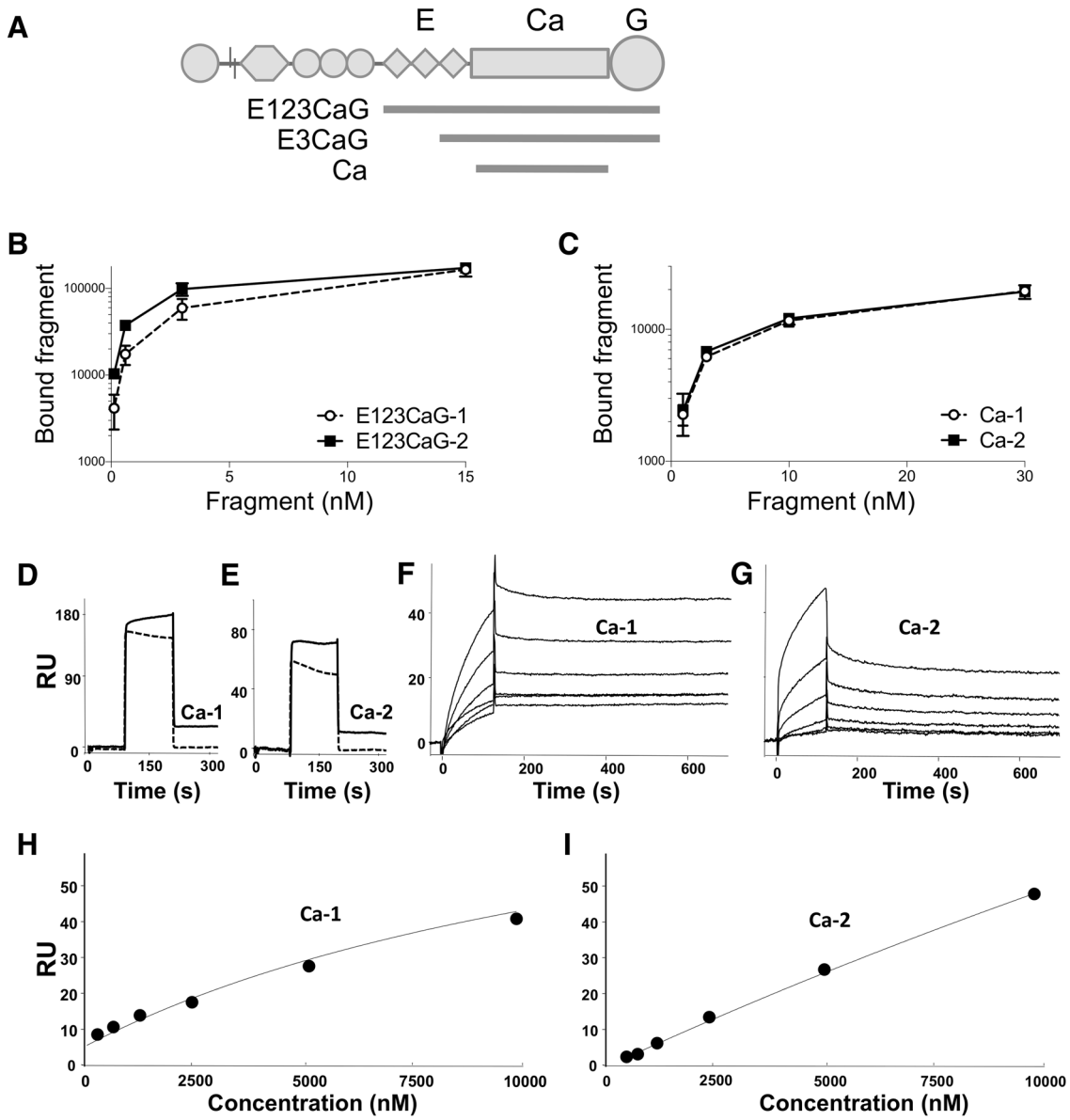

Fig. 2 Localization of the FGF2-binding site in the type III repeats of TSP-2. **a** Schematic representation of TSP-1/TSP-2 and the recombinant fragments analyzed in this study. **b**, **c** Solid-phase assay: binding of biotinylated E123CaG-1 and E123CaG-2 (**b**) and Ca-1 and Ca-2 (**c**) to immobilized FGF2. Data are expressed as specific binding to FGF2 (absorbance, mean and SD, from one experiment representative of 2–3), after subtraction of non-specific binding to BSA-saturated plastic (shown in Suppl Fig. 2). **d**–**g** SPR analysis: sensorgrams showing the binding of Ca-1 (**d**) or Ca-2 (**e**) (both at 100 nM) to FGF2-coated or void sensorchips (straight and dashed lines, respectively). Representative blank-subtracted sensorgrams overlays showing the binding of increasing concentrations of Ca-1 (**f**) or of Ca-2 (**g**) to the FGF2-coated sensorchip. **h**, **i** Saturation curves obtained using the values of RU bound at equilibrium from injections of increasing concentrations of Ca-1 or Ca-2, respectively, onto the FGF2-coated sensorchip

TSP-2 affects the interaction of FGF2 with its receptors

We previously demonstrated that the engagement of the heparin-binding site of FGF2 by TSP-1-based small molecules prevented the interaction of FGF2 with HSPG by direct competition, but it also induced long-range dynamics perturbations of the FGF2 molecules, affecting the FGFR-1-binding region and preventing the interaction of FGF2 with its tyrosine kinase receptor FGFR-1 [29, 30]. This, along with the above finding that also TSP-2 interacts with the heparin-binding site of FGF2, prompted us to compare the effect of type III repeats fragments derived from both TSP-1 and 2 on the binding of FGF2 to FGFR-1 [37] and HSPGs [38] using SPR analysis with well-established competition models [39, 40]. As shown in Fig. 4a, E3CaG-2

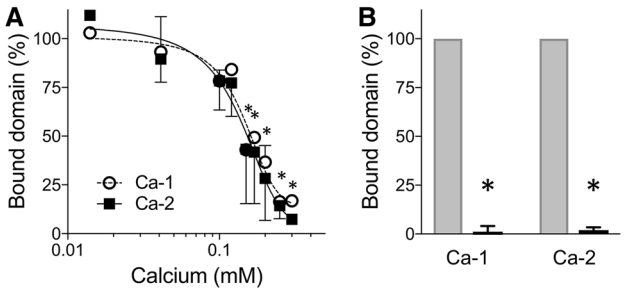

Fig. 3 Effect of calcium and heparin on the binding of TSP-1 and TSP-2 fragments to FGF2. Binding of 5 nM biotin-labeled Ca-1 and Ca-2 to FGF2 was analyzed in the presence of increasing concentration of $CaCl_2$ (**a**) or 1 µg/ml heparin (**b**; gray column, control; black columns, heparin). Data are expressed as the percentage of control binding (in calcium-free buffer), mean and SD of data from one experiment representative of three. $*p < 0.001$ compared to control (ANOVA followed by Bonferroni test)

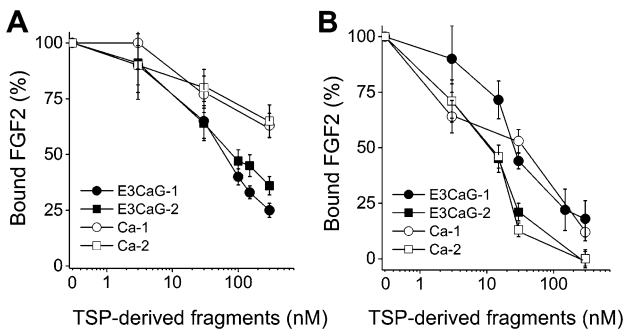

Fig. 4 Inhibitory activity of TSP-1 and TSP-2 fragments on the binding of FGF2 to heparin/HSPGs or FGFR-1. FGF2 was injected over heparin (**a**) or FGFR-1 (**b**) immobilized to the SPR sensorchip in the absence or in the presence of increasing concentrations of the indicated fragment. The amount of FGF2 bound to the surfaces in the different experimental conditions was then measured. Data are expressed as percentage of bound FGF2 (mean and SD of 3 experiments) compared to control (in the absence of competitors)

Table 2 Inhibitory effect of TSP-1 and TSP-2 recombinant fragments on FGF2 interaction with heparin and FGFR-1

Fragment	IC_{50} (nM)	
	Heparin	FGFR-1
E3CaG-1	63.5 ± 15.6	27.2 ± 4.1
E3CaG-2	79.5 ± 26.6	12.4 ± 5.6
Ca-1	> 300	35.8 ± 14.2
Ca-2	> 300	12.7 ± 5.7

SPR analysis was used to evaluate the capacity of the indicated TSP fragments to prevent the binding of FGF2 to sensorchip-immobilized heparin (a HSPG analog used as predictive of the FGF2/HSPGs interaction in cellular models [39, 40]), or FGFR-1. The results shown are the mean and SD of 3–4 independent analysis

and Ca-2 prevented the binding of FGF2 to immobilized heparin (Fig. 4a), here used as a structural analog of HSPGs [39, 40] with IC_{50} that are very similar to those calculated in the same experimental conditions for the corresponding fragments from TSP-1 (Table 2). The two TSP-2-derived fragments were also able to inhibit the binding of FGF2 to immobilized FGFR-1 (Fig. 4b). Again, the IC_{50} values of these inhibitions were comparable to those calculated for the corresponding TSP-1 fragments (Table 2).

Taken together, these findings suggest that, by interacting with the heparin-binding domain of FGF2, also the type III repeats domain of TSP-2 is able to act as dual FGF2 antagonists, inhibiting the interaction of FGF2 with both HSPG and FGFR-1.

Identification of the minimal FGF2 interacting sequence on TSP-1 and TSP-2

We previously found that the FGF2-binding site of TSP-1 is located in a sequence of 15 residues (DDDDDNDKIPDDRDN, DD15 peptide, position 739–753) within the 3C repeat of the type III repeats domain [25]. MD simulations and NMR data indicated that the highest number of contacts was between K746 and D752 [25]. This knowledge was used to guide the identification of a smaller, minimal recognition sequence in both TSP-1 and TSP-2.

To identify the minimal active sequence of TSP-1, the FGF2-binding ability of biotinylated synthetic peptides covering different portions of the DD15 sequence (Fig. 5a) was tested. Peptide KIPDDRD (746–752), although not as potent as the entire DD15 peptide, retained the ability to bind FGF2 (Fig. 5b). In contrast, peptide KIPDD and peptide DDDNDKIPDD (containing the potentially involved residue D741 but lacking R751 and D752) did not show any appreciable binding, indicating that residues R751 and D752, but not D741, are necessary for the interaction.

We next investigated whether the TSP-2 sequence GVTDEKD (residues 748–754, Suppl Fig. 5a), corresponding to the KIPDDRD sequence of TSP-1, was also active in binding FGF2. The two sequences share two conserved D residues and three conservative substitutions (I–V, D–E, and R–K) thus displaying only 2 (out of 7) non-conservative substitutions. The GVTDEKD peptide from TSP2 effectively bound FGF2 in a manner that is indistinguishable from TSP-1-derived KIPDDRD (Fig. 5c).

Basic Local Alignment Search Tool (BLAST) search identified a second sequence located in the 11C repeat of TSP-1 (IPDDKD, residues 903–908) with high similarity with KIPDDRD, (with only one non-conservative K–G substitution and one conservative R–K substitution, Suppl Fig. 5a). We then investigated the FGF2-binding ability of this sequence as well as of the conserved corresponding sequence in TSP-2 (VPDDRD, residues 905–910),

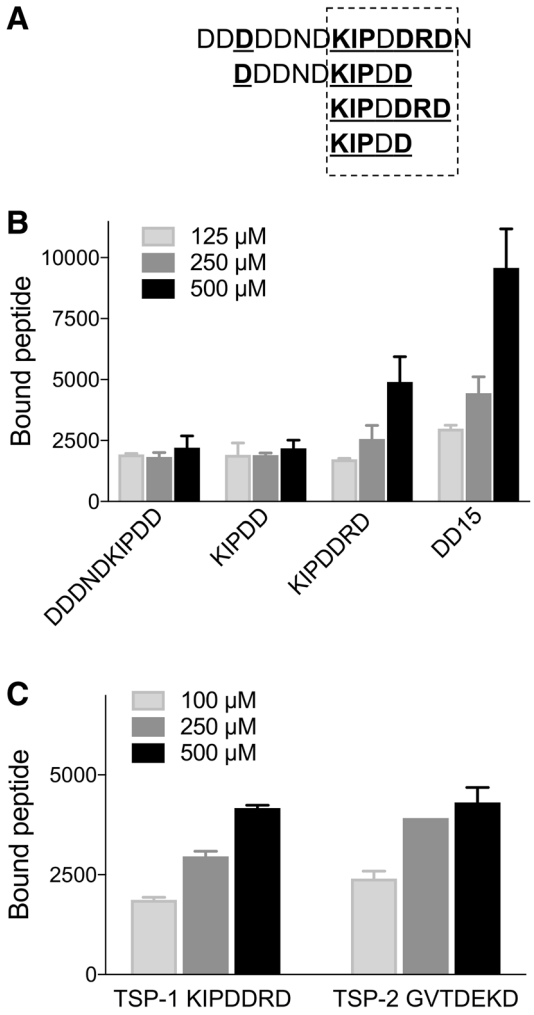

Fig. 5 Identification of the minimal FGF2 binding sequence on TSP-1 and TSP-2. **a** Sequence of the synthetic peptides of TSP-1 (top: DD15 peptide, position 739–753). Bold and underlined are the residues making contact with FGF2 according to [25]. The dotted box indicates the peptide segment (K746-D752) showing the highest number of contacts. **b** Binding of biotinylated peptides to FGF2, identifying KIPDDRD as the minimal FGF2 binding sequence of TSP-1. **c** FGF2-binding ability of TSP-1 KIPDDRD and the corresponding sequence on TSP-2, GVTDEKD. Data are mean and SD of triplicates from one experiment representative of at least 3

presenting only a non-conservative P–T substitution. Both the peptides were able to bind FGF2 (Suppl Fig. 5b).

Computational analysis of TSP-1- and TSP-2-derived peptides

We further analyzed the conformation of the active TSP1 and TSP2 peptides by molecular dynamics simulations, and their structural determinants for FGF2 recognition by docking calculations.

All atom molecular dynamics simulations of KIPDDRD (from TSP-1) and GVTDEKD (from TSP-2) peptides in explicit solvent showed that they both assume preferentially four conformations that cover ~ 90% of the all conformations visited during the dynamics (Suppl Results and Suppl Fig. 6): (1) The backbone is extended, with different variants in the positions of the side chains. This is the most visited conformation. Most of the differences are observed in the arrangement of the side chains of the segment 748–750 of the peptide from TSP-1 and the corresponding TSP-2 segment 746–748, which has two non-conservative substitutions. (2) The backbone is partially folded due to intra-ligand hydrogen bonds connecting the backbone of different residues. (3) The backbones of both peptides assume a helical-like shape. (4) The backbones assume a semi-extended conformation at their ends.

Both peptides, in their principal conformations, were next docked onto the FGF2 crystal structure (Fig. 6a, b). The results indicated that they can both engage the same two sites on the FGF2 surface. One site partially overlaps with the heparin-binding site of FGF2 and both ligands can establish favorable coupling interactions between their negatively charged Asp/Glu groups and the Lys sidechains of FGF2 (Fig. 6a). The other one totally overlaps with the FGF2 heparin-binding site and, besides establishing favorable electrostatic interactions between charged groups, these binding poses also optimize the hydrophobic interactions of Ile747 and Pro748 in the TSP-1-derived peptide and Val749 in TSP-2-derived peptide (Fig. 6b). Interestingly, the conformations assumed by both peptides in complex with FGF2 are very similar to each other and they are in good agreement, from the structural standpoint, with the representative structure of the most populated cluster discussed above, obtained from molecular dynamics simulations (Fig. 6c,d).

Summing up, explicit solvent molecular dynamics simulations of both peptides suggest that they preferentially assume four conformations. The majority of the conformations visited show a spatial coincidence among the functional groups of the peptides. A moderate variability was observed for the positions of the side chains of residues Asp752(TSP-1) and Asp754(TSP-2) and Arg751(TSP-1)/Lys753(TSP-2). Higher variability was observed for residues 748–750 of the peptide from TSP-1 and the corresponding TSP-2 segment 746–748. Complexes of these peptides and FGF2 generated with docking runs support the hypothesis that they are both able to bind FGF2 with comparable binding properties.

Cross-inhibitory effect of TSP-1-derived non-peptidic compounds on TSP-2/FGF2 interaction

A pharmacophore-based screening approach has previously led to the identification of non-peptidic small molecules that reproduce the structure of the FGF2 binding sequence of TSP-1. The compounds bound FGF2 and inhibited FGF2/TSP-1 interaction [25, 29]. We used them as tools to confirm

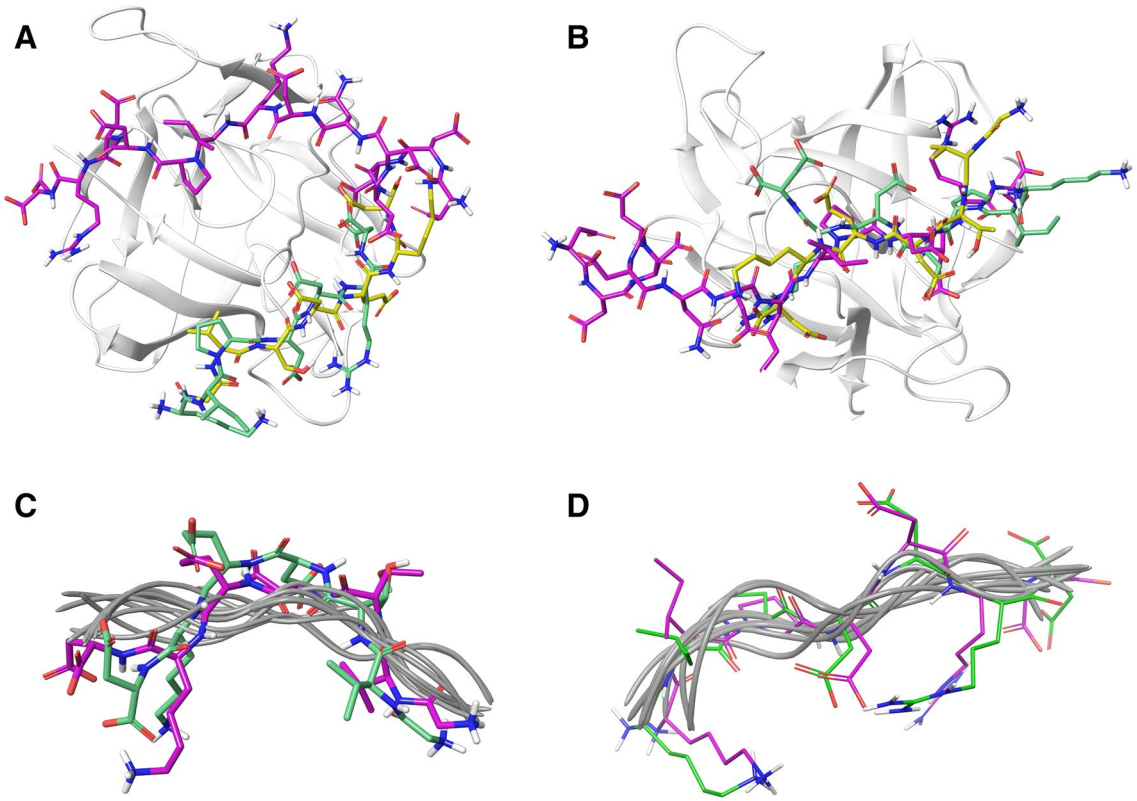

Fig. 6 Computational analysis of TSP-1- and TSP-2-derived peptides. **a** and **b** Superposition of the docking poses of the KIPDDRD (green) and GVTDEKD (yellow) peptide on the FGF2 heparin (pink) binding surface. **a** and **b** The two sites of interaction. **c** and **d** Superposition of the backbone of the docking poses and the most populated conformation obtained from molecular dynamics (pink). Backbones have been colored in gray. As a comparison with the most populated conformation, the side chain of one docking pose (green) has been reported

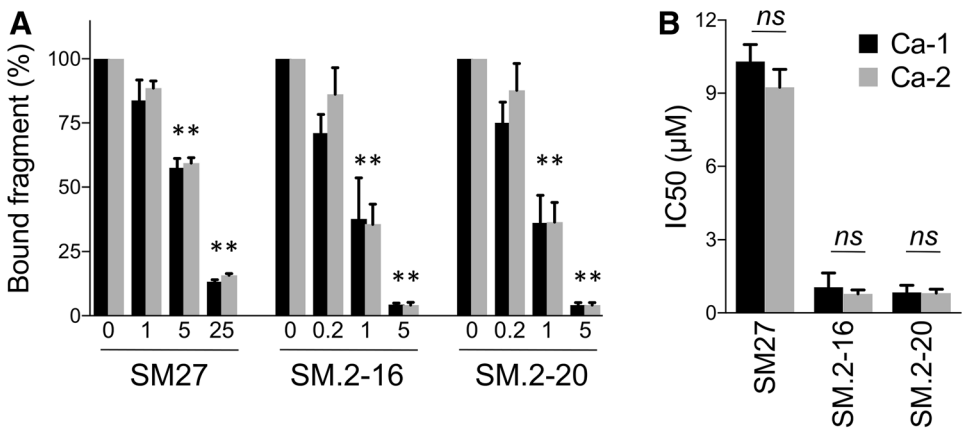

Fig. 7 Competition of TSP-1-mimetic small molecules for Ca-1 and Ca-2 binding to FGF2. Binding of 5 nM biotinylated Ca-1 and Ca-2 domains to FGF2 in the presence of the indicated concentration (μM) of SM27, SM.2–16, or SM.2–20. Data are the percentage of control binding (**a**), and IC_{50} values (**b**), mean and SE of values from 3 experiments. $*p < 0.0001$ compared to control (ANOVA followed by Bonferroni test)

the similarity in the recognition determinants of TSP-1 and TSP-2. The initial hit SM27 [25] and second-generation, more potent compounds SM.2–16 and SM.2–20 [29] prevented the binding of the Ca-2 domain to FGF2, with a similar IC_{50} compared to Ca-1 (Fig. 7). This confirms that the type III repeats domains of TSP-1 and TSP-2 share the same structural and conformational determinants required for FGF2 recognition.

Discussion

Both TSP-1 and TSP-2 are major endogenous inhibitors of angiogenesis. We previously demonstrated that binding and sequestration of FGF2 is a mechanism of the antiangiogenic activity of TSP-1. The high structural similarity between TSP-2 and TSP-1 and the ability of TSP-2 to inhibit FGF2 angiogenic activity [5, 6] prompted us to evaluate the possibility that, similarly to TSP-1, also TSP-2 might interact with FGF2.

This study demonstrates that TSP-2 binds to FGF2, similarly to TSP-1 and with comparable binding properties. Both TSPs have high affinity for FGF2 (*Kd* in the nM range) and recognize the heparin-binding domain of FGF2 through a sequence located in the calcium-binding type III repeats domain. Similar to TSP1, binding of TSP-2 to FGF2 is affected by calcium, in agreement with the known, profound effects of calcium on the type III repeats structure and exposure of active sequences. Indeed, in physiological conditions, the concentration of calcium in the extracellular space (in the millimolar range) maintains a folded conformation of TSP-1, making the exposure of the FGF2-binding domain unlikely. Similarly, another active sequence present in this domain, the cell adhesive RGD motif, is cryptic in calcium-loaded TSP-1, and becomes exposed by lowering calcium, or by exposure to reducing agents [34] or in the presence of secreted disulfide isomerase [45]. It is therefore possible that different mechanisms control the exposure of the FGF2-binding site, including local fluctuation in calcium concentration and activity of protein thiol isomerases in the extracellular space. Moreover, it could also be hypothesized a role for TSP ligands affecting the molecule conformation and the activity of protease that release bioactive small fragments of TSP-1.

The type III repeats are part of the signature domain of TSPs, highly conserved in all the members of the TSP family. Little is known on the regulation of angiogenesis and FGF2 activity by the other TSPs (TSP-3, TSP-4, and COMP), although TSP-4 has been reported to promote angiogenesis via the integrin α_2 and the gabapentin receptor $\alpha_2\delta$-1 on endothelial cells [41]. Interestingly, TSP-3 and TSP-4 contain 4-residue inserts in 11C [1]. The insert would be predicted to disrupt the interaction with FGF2. Nonetheless, the conservation of the signature domain among the TSP family members calls for further studies to investigate the FGF2-binding capacity of other TSPs.

The similarity between the two TSPs holds also at a structural level, when the FGF2-binding domain in the two molecules is tracked down to short amino acid sequences. Indeed, two heptapeptides, corresponding to the TSP-1 sequence KIPDDRD (746–752) and the corresponding TSP-2 sequence GVTDEKD (748–754) in the 3C repeat, retain the capacity to bind FGF2. BLAST analysis identified another putative FGF2 binding sequence in the 11C repeat of TSP-1 and TSP-2. In both TSPs, the 11C repeat is part of the 10N–13C hairpin loop that interacts with the 2nd and 3rd EGF-like type II repeats [1, 34, 42]. The relative accessibility of the 3C and 11C sequences to FGF2 at different calcium concentrations are not known. This and the relative role of the two sequences in mediating TSP interaction with FGF2 warrant further investigation.

TSP-1 and TSP-2 share similar conformation and structural determinants for FGF2 recognition. Explicit solvent molecular dynamics simulations showed that both peptides assume similar preferential conformations, with spatial coincidence among the functional groups. Moreover, docking analysis indicated that the two peptides can interact with the heparin-binding site of FGF2, as previously reported for the 15-mer peptide of TSP-1 [25]. In particular, both peptides have the same two putative binding sites and they can establish similar interactions. The structural similarity of the FGF2-recognition site in the two TSPs was confirmed experimentally, by the finding that FGF2-binding small molecules that retain the structural and functional properties of the FGF2-binding site of TSP-1 [25, 29] were able to prevent TSP-2 interaction with FGF2, with potency similar to that observed for TSP-1.

A direct correlation exists between the length of the TSP-derived fragments and their affinity for FGF2 (intact TSP > E123CaG > Ca). The possibility that the trimeric structure of intact TSP might somehow affect the affinity is unlikely, since modeling studies and NMR spectroscopy indicated that a single binding site for type III sequences is present in FGF2 [25]. Moreover, binding affinity is sensibly reduced also when passing from monomeric large *C*-terminal fragments (E123CaG) to smaller Ca fragments, supporting the concept that an important contribution to FGF2/TSP interaction derives from flanking amino acid sequences.

The interaction of TSP-2 and TSP-1 with FGF2 has similar and significant effects on the interaction of the growth factor with its proangiogenic receptors. We found that the FGF2-binding fragments of TSP-2 prevented the binding of FGF2 to both heparin and FGFR-1. Similar to TSP-1, inhibition of binding to heparin/HSPG is caused by direct competition due to engagement of the heparin-binding site of FGF2, as also supported by the observation that heparin abolished TSP-2/FGF2 interaction. On the other hand, inhibition of FGF2 binding to FGFR-1 indicates that also TSP-2 can act with an allosteric mechanism, by inducing the dynamics perturbations of distant residues of FGF2 directly involved in the FGFR-1 binding (at the D2 and D3 domains and D2-D3 linker), as previously demonstrated for TSP-1-based small molecules [29, 30]. This simultaneous, double mechanism of action is particularly important since FGF2 signaling requires the formation of a productive ternary

complex composed by FGF2 itself, FGFR, and HPSG [43, 44].

Despite the similarities in structure and antiangiogenic function, TSP-1 and TSP-2 present relevant differences. They diverge in the spatio-temporal pattern of expression in embryo and adult tissues [2, 45, 46]. Moreover, while TSP-1 is a major product of platelets and inflammatory and endothelial cells, TSP-2 is mainly produced by fibroblasts [47]. The two TSPs present a different time course of expression after injury [48], and also can differ in their mechanisms of action. For example, in contrast to TSP-1, TSP-2 is a weaker activator of CD47 [19]. Importantly, in contrast to TSP-1, TSP-2 does not activate TGFβ [49] and can actually inhibit TSP-1-mediated activation of TGFβ [50]. The fact that, despite the above differences, TSP-1 and 2 have evolutionary retained a common antiangiogenic activity and in particular a FGF2-antagonist capacity mediated by a conserved mechanism represents an example of biochemical redundancy and sustains the importance of TSPs in the regulation of the angiogenic process.

Both TSP-1 and TSP-2 have been proposed as templates to guide the design of antiangiogenic agents for antineoplastic therapy [2, 4, 51]. The TSP-2-based N-TSP2-Fc, an *N*-terminal recombinant fragment of TSP-2 fused with the IgG-Fc1 fragment, prevented angiogenesis via CD36 and reduced the in vivo growth of breast cancer models [52]. FGF2 is a relevant target for therapies to treat pathologies based on FGF-driven cell proliferation and angiogenesis, including cancer, where FGF2 simultaneously affects angiogenesis, tumor cells, and the stroma compartment [43, 44]. The recognition of TSP-2 as ligand and regulator of FGF2 bioavailability supports the possibility to develop new inhibitors of angiogenesis and FGF2-driven pathologies based on this matricellular protein.

Funding Supported by the Italian Association for Cancer Research (AIRC IG16833 to GT), Ministero dell'Istruzione, Università e Ricerca (MIUR, ex 60%) to MR.

Compliance with ethical standards

Conflict of interest The authors declare no conflicts of interest.

References

1. Carlson CB, Lawler J, Mosher DF (2008) Structures of thrombospondins. Cell Mol Life Sci 65:672–686
2. Adams JC, Lawler J (2011) The thrombospondins. Cold Spring Harb Perspect Biol 3:a009712. https://doi.org/10.1101/cshperspect.a009712
3. Armstrong LC, Bornstein P (2003) Thrombospondins 1 and 2 function as inhibitors of angiogenesis. Matrix Biol 22:63–71
4. Lawler PR, Lawler J (2012) Molecular basis for the regulation of angiogenesis by thrombospondin-1 and -2. Cold Spring Harb Perspect Med 2:a006627. https://doi.org/10.1101/cshperspect.a006627
5. Volpert OV, Tolsma SS, Pellerin S et al (1995) Inhibition of angiogenesis by thrombospondin-2. Biochem Biophys Res Commun 217:326–332. https://doi.org/10.1006/bbrc.1995.2780
6. Panetti TS, Chen H, Misenheimer TM et al (1997) Endothelial cell mitogenesis induced by LPA: inhibition by thrombospondin-1 and thrombospondin-2. J Lab Clin Med 129:208–216
7. Armstrong LC, Björkblom B, Hankenson KD et al (2002) Thrombospondin 2 inhibits microvascular endothelial cell proliferation by a caspase-independent mechanism. Mol Biol Cell 13:1893–1905
8. Kyriakides TR, Zhu YH, Smith LT et al (1998) Mice that lack thrombospondin 2 display connective tissue abnormalities that are associated with disordered collagen fibrillogenesis, an increased vascular density, and a bleeding diathesis. J Cell Biol 140:419–430
9. Kyriakides TR, Tam JW, Bornstein P (1999) Accelerated wound healing in mice with a disruption of the thrombospondin 2 gene. J Invest Dermatol 113:782–787. https://doi.org/10.1046/j.1523-1747.1999.00755.x
10. Hawighorst T, Velasco P, Streit M et al (2001) Thrombospondin-2 plays a protective role in multistep carcinogenesis: a novel host anti-tumor defense mechanism. EMBO J 20:2631–2640. https://doi.org/10.1093/emboj/20.11.2631
11. Kunstfeld R, Hawighorst T, Streit M et al (2014) Thrombospondin-2 overexpression in the skin of transgenic mice reduces the susceptibility to chemically induced multistep skin carcinogenesis. J Dermatol Sci 74:106–115. https://doi.org/10.1016/j.jdermsci.2014.01.002
12. Sun R, Wu J, Chen Y et al (2014) Down regulation of Thrombospondin2 predicts poor prognosis in patients with gastric cancer. Mol Cancer 13:225. https://doi.org/10.1186/1476-4598-13-225
13. Tokunaga T, Nakamura M, Oshika Y et al (1999) Thrombospondin 2 expression is correlated with inhibition of angiogenesis and metastasis of colon cancer. Br J Cancer 79:354–359. https://doi.org/10.1038/sj.bjc.6690056
14. Oshika Y, Masuda K, Tokunaga T et al (1998) Thrombospondin 2 gene expression is correlated with decreased vascularity in non-small cell lung cancer. Clin Cancer Res 4:1785–1788
15. Dvorkina M, Nieddu V, Chakelam S et al (2016) A Promyelocytic leukemia protein-thrombospondin-2 axis and the risk of relapse in neuroblastoma. Clin Cancer Res 22:3398–3409. https://doi.org/10.1158/1078-0432.CCR-15-2081
16. Chijiwa T, Abe Y, Ikoma N et al (2009) Thrombospondin 2 inhibits metastasis of human malignant melanoma through microenvironment-modification in NOD/SCID/gammaCnull (NOG) mice. Int J Oncol 34:5–13
17. Streit M, Riccardi L, Velasco P et al (1999) Thrombospondin-2: a potent endogenous inhibitor of tumor growth and angiogenesis. Proc Natl Acad Sci USA 96:14888–14893
18. Simantov R, Febbraio M, Silverstein RL (2005) The antiangiogenic effect of thrombospondin-2 is mediated by CD36 and modulated by histidine-rich glycoprotein. Matrix Biol 24:27–34. https://doi.org/10.1016/j.matbio.2004.11.005
19. Isenberg JS, Annis DS, Pendrak ML et al (2009) Differential interactions of thrombospondin-1, -2, and -4 with CD47 and effects on cGMP signaling and ischemic injury responses. J Biol Chem 284:1116–1125. https://doi.org/10.1074/jbc.M804860200
20. Calabro NE, Kristofik NJ, Kyriakides TR (2014) Thrombospondin-2 and extracellular matrix assembly. Biochim Biophys Acta 1840:2396–2402. https://doi.org/10.1016/j.bbagen.2014.01.013
21. Resovi A, Pinessi D, Chiorino G, Taraboletti G (2014) Current understanding of the thrombospondin-1 interactome. Matrix Biol 37:83–91. https://doi.org/10.1016/j.matbio.2014.01.012

22. Margosio B, Marchetti D, Vergani V et al (2003) Thrombospondin 1 as a scavenger for matrix-associated fibroblast growth factor 2. Blood 102:4399–4406
23. Margosio B, Rusnati M, Bonezzi K et al (2008) Fibroblast growth factor-2 binding to the thrombospondin-1 type III repeats, a novel antiangiogenic domain. Int J Biochem Cell Biol 40:700–709
24. Taraboletti G, Belotti D, Borsotti P et al (1997) The 140-kilodalton antiangiogenic fragment of thrombospondin-1 binds to basic fibroblast growth factor. Cell Growth Differ 8:471–479
25. Colombo G, Margosio B, Ragona L et al (2010) Non-peptidic thrombospondin-1 mimics as fibroblast growth factor-2 inhibitors: an integrated strategy for the development of new antiangiogenic compounds. J Biol Chem 285:8733–8742. https://doi.org/10.1074/jbc.M109.085605
26. Annis DS, Murphy-Ullrich JE, Mosher DF (2006) Function-blocking antithrombospondin-1 monoclonal antibodies. J Thromb Haemost 4:459–468
27. Mosher DF, Huwiler KG, Misenheimer TM, Annis DS (2002) Expression of recombinant matrix components using baculoviruses. Methods Cell Biol 69:69–81
28. Amblard M, Fehrentz J-A, Martinez J, Subra G (2006) Methods and protocols of modern solid phase peptide synthesis. Mol Biotechnol 33:239–254. https://doi.org/10.1385/MB:33:3:239
29. Foglieni C, Pagano K, Lessi M et al (2016) Integrating computational and chemical biology tools in the discovery of antiangiogenic small molecule ligands of FGF2 derived from endogenous inhibitors. Sci Rep 6:23432. https://doi.org/10.1038/srep23432
30. Pagano K, Torella R, Foglieni C et al (2012) Direct and allosteric inhibition of the FGF2/HSPGs/FGFR1 ternary complex formation by an antiangiogenic, thrombospondin-1-mimic small molecule. PLoS ONE 7:e36990. https://doi.org/10.1371/journal.pone.0036990
31. Misenheimer TM, Mosher DF (2005) Biophysical characterization of the signature domains of thrombospondin-4 and thrombospondin-2. J Biol Chem 280:41229–41235. https://doi.org/10.1074/jbc.M504696200
32. Misenheimer TM, Hannah BL, Annis DS, Mosher DF (2003) Interactions among the three structural motifs of the C-terminal region of human thrombospondin-2. Biochemistry 42:5125–5132
33. Carlson CB, Bernstein DA, Annis DS et al (2005) Structure of the calcium-rich signature domain of human thrombospondin-2. Nat Struct Mol Biol 12:910–914
34. Kvansakul M, Adams JC, Hohenester E (2004) Structure of a thrombospondin C-terminal fragment reveals a novel calcium core in the type 3 repeats. Embo J 23:1223–1233
35. Hannah BL, Misenheimer TM, Annis DS, Mosher DF (2003) A polymorphism in thrombospondin-1 associated with familial premature coronary heart disease causes a local change in conformation of the Ca^{2+}-binding repeats. J Biol Chem 278:8929–8934
36. Hannah BL, Misenheimer TM, Pranghofer MM, Mosher DF (2004) A polymorphism in thrombospondin-1 associated with familial premature coronary artery disease alters Ca^{2+} binding. J Biol Chem 279:51915–51922
37. Giacomini A, Chiodelli P, Matarazzo S et al (2016) Blocking the FGF/FGFR system as a "two-compartment" antiangiogenic/antitumor approach in cancer therapy. Pharmacol Res 107:172–185. https://doi.org/10.1016/j.phrs.2016.03.024
38. Chiodelli P, Bugatti A, Urbinati C, Rusnati M (2015) Heparin/Heparan sulfate proteoglycans glycomic interactome in angiogenesis: biological implications and therapeutical use. Molecules 20:6342–6388. https://doi.org/10.3390/molecules20046342
39. Rusnati M, Presta M (2015) Angiogenic growth factors interactome and drug discovery: the contribution of surface plasmon resonance. Cytokine Growth Factor Rev 26:293–310. https://doi.org/10.1016/j.cytogfr.2014.11.007
40. Rusnati M, Bugatti A, Mitola S et al (2009) Exploiting surface plasmon resonance (SPR) technology for the identification of fibroblast growth factor-2 (FGF2) antagonists endowed with antiangiogenic activity. Sensors (Basel) 9:6471–6503. https://doi.org/10.3390/s90806471
41. Muppala S, Frolova E, Xiao R et al (2015) Proangiogenic properties of thrombospondin-4. Arterioscler Thromb Vasc Biol 35:1975–1986. https://doi.org/10.1161/ATVBAHA.115.305912
42. Annis DS, Gunderson KA, Mosher DF (2007) Immunochemical analysis of the structure of the signature domains of thrombospondin-1 and thrombospondin-2 in low calcium concentrations. J Biol Chem 282:27067–27075. https://doi.org/10.1074/jbc.M703804200
43. Turner N, Grose R (2010) Fibroblast growth factor signalling: from development to cancer. Nat Rev Cancer 10:116–129. https://doi.org/10.1038/nrc2780
44. Wesche J, Haglund K, Haugsten EM (2011) Fibroblast growth factors and their receptors in cancer. Biochem J 437:199–213. https://doi.org/10.1042/BJ20101603
45. Stenina-Adognravi O (2014) Invoking the power of thrombospondins: regulation of thrombospondins expression. Matrix Biol 37:69–82. https://doi.org/10.1016/j.matbio.2014.02.001
46. Tooney PA, Sakai T, Sakai K et al (1998) Restricted localization of thrombospondin-2 protein during mouse embryogenesis: a comparison to thrombospondin-1. Matrix Biol 17:131–143
47. Kyriakides TR, Maclauchlan S (2009) The role of thrombospondins in wound healing, ischemia, and the foreign body reaction. J Cell Commun Signal 3:215–225. https://doi.org/10.1007/s12079-009-0077-z
48. Agah A, Kyriakides TR, Lawler J, Bornstein P (2002) The lack of thrombospondin-1 (TSP1) dictates the course of wound healing in double-TSP1/TSP2-null mice. Am J Pathol 161:831–839. https://doi.org/10.1016/S0002-9440(10)64243-5
49. Murphy-Ullrich JE, Suto MJ (2017) Thrombospondin-1 regulation of latent TGF-β activation: a therapeutic target for fibrotic disease. Matrix Biol. https://doi.org/10.1016/j.matbio.2017.12.009
50. Schultz-Cherry S, Chen H, Mosher DF et al (1995) Regulation of transforming growth factor-b activation by discrete sequences of thrombospondin 1. J Biol Chem 270:7304–7310
51. Taraboletti G, Rusnati M, Ragona L, Colombo G (2010) Targeting tumor angiogenesis with TSP-1-based compounds: rational design of antiangiogenic mimetics of endogenous inhibitors. Oncotarget 1:662–673
52. Koch M, Hussein F, Woeste A et al (2011) CD36-mediated activation of endothelial cell apoptosis by an N-terminal recombinant fragment of thrombospondin-2 inhibits breast cancer growth and metastasis in vivo. Breast Cancer Res Treat 128:337–346. https://doi.org/10.1007/s10549-010-1085-7